Geophysical Research Letters

RESEARCH LETTER
10.1029/2023GL104246

Key Points:

- We present signal-to-noise calculations of stratospheric ozone depletion in chemistry-climate models relative to 1960–1970
- Statistically significant ozone depletion does not emerge in 1980, which is traditionally used as a benchmark for ozone recovery
- In most regions de-emergence occurs before ozone returns to 1980 levels except in Antarctica where de-emergence occurs 25 years later

Supporting Information:

Supporting Information may be found in the online version of this article.

Correspondence to:

L. E. Revell,
laura.revell@canterbury.ac.nz

Citation:

Robertson, F., Revell, L. E., Douglas, H., Archibald, A. T., Morgenstern, O., & Frame, D. (2023). Signal-to-noise calculations of emergence and de-emergence of stratospheric ozone depletion. *Geophysical Research Letters*, *50*, e2023GL104246. https://doi.org/10.1029/2023GL104246

Received 25 APR 2023
Accepted 12 AUG 2023

Author Contributions:

Conceptualization: L. E. Revell
Formal analysis: F. Robertson, O. Morgenstern
Funding acquisition: D. Frame
Investigation: F. Robertson, L. E. Revell, A. T. Archibald
Methodology: L. E. Revell, H. Douglas
Software: F. Robertson
Supervision: L. E. Revell
Validation: H. Douglas
Visualization: F. Robertson
Writing – original draft: F. Robertson, L. E. Revell

Signal-To-Noise Calculations of Emergence and De-Emergence of Stratospheric Ozone Depletion

F. Robertson[1], L. E. Revell[1], H. Douglas[2], A. T. Archibald[3,4], O. Morgenstern[5], and D. Frame[1,6]

[1]School of Physical and Chemical Sciences, University of Canterbury, Christchurch, New Zealand, [2]New Zealand Climate Change Research Institute, Victoria University of Wellington Te Herenga Waka, Wellington, New Zealand, [3]Yusuf Hamied Department of Chemistry, University of Cambridge, Cambridge, UK, [4]National Centre for Atmospheric Science, Cambridge, UK, [5]National Institute of Water and Atmospheric Research, Wellington, New Zealand, [6]School of Earth and Environment, University of Canterbury, Christchurch, New Zealand

Abstract The year when total column ozone (TCO) returns to 1980 levels is commonly used to quantify recovery from disturbance caused by ozone-depleting substances. This date is reasonable but somewhat arbitrary. Here we borrow an indicator from climate change research, the signal-to-noise (S/N) metric to investigate how TCO might return to statistically similar levels to those of the pre-ozone hole era (1960–1970). We calculate S/N for ozone projections from the Chemistry-Climate Model Initiative. In most regions, a return to 1980 levels doesn't represent TCO recovery to pre-disturbance conditions because it does not account for internal variability or reflect when statistically significant TCO losses occurred. Future projections show that, in most regions, TCO "de-emerges" (i.e., S/N becomes less than one standard deviation from the pre-disturbance mean) before it returns to its 1980 value. We conclude that S/N is an appropriate, perhaps complementary metric for determining when TCO returns to a pre-disturbance state.

Plain Language Summary The stratospheric ozone layer is expected to recover from the damaging effects of chlorofluorocarbons (CFCs) and other halogen-containing source gases this century. Ozone recovery is traditionally but somewhat arbitrarily defined as the year when total column ozone (TCO) abundances return to 1980 levels. Here, we use a metric commonly used in the climate change emergence literature—signal-to-noise (S/N)—to quantify statistically significant changes in TCO in models and observations relative to a period before CFC-induced ozone depletion began. The S/N framing ties recovery to unperturbed environmental conditions, rather than to the environment in a specific year. We argue that tying recovery to unperturbed local environmental conditions is at least as reasonable as tying it to the same global date. Our calculations, which account for natural variability, show that 1980 does not reflect the onset of statistically significant ozone loss. Using a return of TCO to 1980 levels underestimates the time of recovery in Antarctica, where losses have been most significant, and overestimates the time to recovery in other regions. We conclude that signal-to-noise is a useful metric to assess the return of TCO to its baseline state and evaluate the effectiveness of the Montreal Protocol.

1. Introduction

The stratospheric ozone layer, which protects the biosphere against harmful UV-B radiation, was severely damaged by halogen-containing source gases emitted in the late 20th century. Owing to the success of the Montreal Protocol (1987) and its subsequent Adjustments and Amendments, signs of ozone recovery are appearing (Coldewey-Egbers et al., 2022; Solomon et al., 2016; Weber et al., 2022). Ozone recovery is typically defined as the date at which total column ozone (TCO) returns to 1980 levels (Hassler & Young, 2022). The most recent WMO Scientific Assessment of Ozone Depletion states that near-global (60°N–60°S) TCO is projected to return to 1980 levels around 2040 (Hassler & Young, 2022).

It has long been recognised that 1980 is not an accurate reflection of when stratospheric ozone depletion began: previous studies have shown that stratospheric ozone depletion was underway prior to 1980, during a period in which tropospheric ozone abundances were increasing (Farman et al., 1985; Langematz et al., 2016; Shepherd et al., 2014; Tarasick et al., 2019). 1980 is used to assess return dates as it marks the beginning of the first decade with continuous satellite TCO observations. In addition, diagnosing "recovery" of the ozone layer is complicated because of the contribution from natural interannual variability, and from the forced response of

Writing – review & editing: H. Douglas, A. T. Archibald, O. Morgenstern, D. Frame

stratospheric ozone, and the stratosphere itself, to increases in atmospheric greenhouse gas (GHG) concentrations (Chipperfield et al., 2017; Morgenstern et al., 2018). Using an ensemble of chemistry-climate models, Eyring et al. (2010) assessed the milestones of ozone returning to historical values, versus ozone no longer being influenced by ozone-depleting substances (ODSs). They showed that upper stratospheric ozone returns to 1980 levels by approximately 2025 as a result of CO_2-cooling of the stratosphere, however, ozone is still influenced by ODSs through the 21st century. In the tropical lower stratosphere, the models simulate continuous decreases in ozone through the 21st century, even once ozone is no longer influenced by ODSs, because of GHG-driven increases in tropical upwelling.

Here, we explore a metric for quantifying ozone recovery which is commonly used in the climate change emergence literature: that of the signal-to-noise ratio (Douglas et al., 2023; Frame et al., 2017; Harrington et al., 2018; Hawkins et al., 2020). Signal-to-noise (S/N) ratios reveal when the trend in a variable of interest emerges above natural variability. We calculate S/N for the historical period and show projections for stratospheric ozone in the 21st century and demonstrate the utility of this metric for defining the emergence and "de-emergence" of stratospheric ozone depletion by long-lived ODSs controlled by the Montreal Protocol.

2. Methods

2.1. Models, Scenarios and Observations

We analyzed simulations performed for the Stratosphere-troposphere Processes and their Role in Climate/International Global Atmospheric Chemistry (SPARC/IGAC) Chemistry-Climate Initiative Phase 1 (CCMI-1; Eyring, Lamarque, et al. (2013); Morgenstern et al. (2017)). We focus on the "future reference" simulation, refC2, which spans 1960–2100 and has previously been used to determine ozone recovery dates (Braesicke et al., 2018; Dhomse et al., 2018). Long-lived chlorine- and bromine-containing ODSs controlled by the Montreal Protocol are prescribed via the WMO A1 scenario (World Meteorological Organization, 2011). Historical GHG concentrations are prescribed until 2005, and follow Representative Concentration Pathway (RCP) 6.0 thereafter (Masui et al., 2011). The refC2 simulations have free-running meteorology, and no volcanic forcing is prescribed (Eyring, Lamarque, et al., 2013). Some models included an interactive ocean, while others used prescribed sea surface temperature and sea ice concentrations (Morgenstern et al., 2017). Previous analyses have shown that historical TCO in the refC2 simulations shows good agreement with observations (Dhomse et al., 2018; Son et al., 2018).

Although ozone projections for a range of GHG scenarios are available via the sixth Climate Model Intercomparison Project (CMIP6; Eyring et al. (2016); Keeble et al. (2021)), most of the CMIP6 models did not calculate ozone via an interactive chemistry scheme and instead prescribed ozone from a pre-computed data set (Checa-Garcia, 2018; Checa-Garcia et al., 2018). However, the pre-computed data set is inconsistent with ozone projections calculated by models with interactive chemistry, particularly under a high GHG emissions scenario (Revell et al., 2022). Only five CMIP6 models used interactive chemistry, and an analysis of 1980-return dates in these five models shows that the small number of models leads to an overly large inter-model spread (Hassler & Young, 2022).

We focus on the CCMI models as they all have interactive chemistry, and therefore future ozone projections are consistent with future emissions and internal model dynamical fields (Hassler & Young, 2022). The CCMI models are also explicitly designed in support of the WMO ozone assessments. We focus on Phase 1 of CCMI rather than Phase 2 (Plummer et al., 2021), due to the size of the CCMI-1 model ensemble. At the time of analysis, 19 models had performed the refC2 simulation for CCMI-1 while only five models had performed the corresponding future reference simulation (refD2) for CCMI-2. In addition, a multi-model set of "fixed GHG" simulations (senC2fGHG) was available from CCMI-1, but not from CCMI-2. The senC2fGHG simulation is identical to refC2 but has GHG concentrations fixed at constant 1960 levels for the duration of the simulation (1960–2100), allowing us to quantify the de-emergence of halocarbon-induced ozone depletion in the absence of GHG influences.

For each model and simulation, we use the TCO variable ("toz") output by the models. To remove the contribution from tropospheric ozone, we also calculate stratospheric column ozone (SCO) by integrating ozone mixing ratios ("vmro3") between the WMO-defined tropopause (the lowest level at which the lapse rate decreases to 2 K km^{-1} or less; World Meteorological Organization (1957)) and the top of the atmosphere. Models, simulations, and the number of realizations performed for each simulation by a given model are shown in Table S1 in

Supporting Information S1. Where multiple realizations for the same model-scenario pair are available, they are averaged to produce an ensemble mean. S/N is then calculated as described in Section 2.2.

To compare modeled S/N with observations, long-running historical TCO data measured by Dobson spectrometers were acquired for three stations: Oxford (UK), Arosa (Switzerland) and Halley (Antarctica) (Brönnimann, 2022; Brönnimann et al., 2003; Farman et al., 1985). Oxford and Arosa data (spanning 1924–2021 and 1926–2012 respectively) are provided by the World Ozone and Ultraviolet Radiation Data Centre (WOUDC) archive. Data for the Halley Station were provided from 1956 to 1985 by the British Antarctic Survey. Signal-to-noise ratios were computed for observations, as described below, using a noise period spanning the year of earliest observation until 1970.

2.2. Signal-To-Noise Calculations

Signal-to-noise (S/N) is defined as the change in a variable relative to a chosen reference baseline period (signal), as a ratio of its baseline variability (noise; Frame et al. (2017)). Here, TCO was smoothed using an 11-year rolling mean for the following regions: global (90°S-90°N), northern midlatitudes (30–60°N), the tropics (30°N-30°S), southern midlatitudes (30–60°S), the Arctic (60–90°N) and Antarctic (60–90°S). A 10-year rolling mean was chosen over polynomial approximation (as used in studies of S/N in temperatures) due it performing better at capturing the depletion and recovery pattern in TCO trends. TCO was annually-averaged, except for the Arctic and Antarctic, where only the months of March and October were analyzed, respectively. The signal in each grid cell is calculated by regressing column ozone against the smoothed regional column ozone. We regress against the regional mean rather than the global mean (as has previously been done for temperature; Frame et al. (2017); Douglas et al. (2023)) due to the different dynamic and chemical processes influencing ozone in various regions (e.g., the springtime polar stratosphere vs. midlatitudes). The mean over the noise period (defined below) is then removed from the smoothed signal in each grid cell to produce the change in column ozone (S, in Dobson units (DU)).

Noise (N, in DU) in each grid cell is defined here as the average deviation of TCO from the signal over the period 1960–1970. Noise is typically calculated over hundreds of years of pre-industrial control simulations (Douglas et al., 2023; Frame et al., 2017), however, such simulations are not available via CCMI. We instead use 1960–1970 as the noise period; see Text S1 in Supporting Information S1 for further details and validation of this approach. Text S2 in Supporting Information S1 describes in further detail how S/N was calculated.

S/N ratios are calculated for each model independently. First, we calculated the one-sigma multi-model mean (MMM1S), where at each grid point, models lying more than one standard deviation from the multi-model mean are excluded (Dhomse et al., 2018; Revell et al., 2018). The number of models excluded at each grid point ranged between 3 and 7, depending on how much variation was present. To obtain the 16th, 50th and 84th percentiles from the MMM1S data set at each grid point, models are ordered from low to high and the model closest to each percentile is selected. In an analysis of surface temperature projections, Frame et al. (2017) describe S/N ratio thresholds of 1, 2 and 3 (i.e., the number of standard deviations from the mean) as "unusual," "unfamiliar" and "unknown" climates. Hawkins et al. (2020) added "inconceivable" for S/N values above 5. Here, we define the "emergence" of ozone depletion to occur when S/N is less than -1 (more than one standard deviation from the mean). We use the term "de-emergence" to describe when TCO S/N ratios pass back above the -1 threshold. This signifies ozone abundances increasing from a state of depletion to within one standard deviation of their typical values prior to widespread emission of halogen source gases, that is, a recovery. Because tropospheric ozone trends may obscure changes in stratospheric ozone (e.g., Eyring, Arblaster, et al. (2013)), we examine SCO S/N ratios in simulations with fixed GHG concentrations to quantify the de-emergence of CFC-induced ozone depletion.

Variations on the choices above could also be defended, and future work may explore the sensitivity of results to different choices around averaging periods, data sets, and precise definitions of signal and noise. In this paper, we simply aim to take a relatively simple approach to the quantification of signal and noise to illustrate how the concept works, and how it yields different thresholds of recovery from a date-based approach.

3. Results and Discussion

3.1. Signal-To-Noise Ratios in Total Column Ozone

In CCMI refC2 simulations, TCO depletion emerges after 1980 in all regions except the Antarctic and southern midlatitudes (Table 1; Figure 1). A small amount of TCO depletion is visible prior to 1980 (Figures 1b, 1d and 1e), however the emergence threshold (S/N < -1) is not reached. Although equivalent effective stratospheric

Table 1
Emergence and De-Emergence of MMM1S TCO in refC2 Simulations, Represented by the Median Year and the 16th and 84th Percentiles in Brackets

Region	Emergence date (S/N < −1)	De-emergence date (S/N > −1)	1980-return date[a]
Global-mean	1989 (1983–N/A)	2015 (N/A–2039)	2049 (2043–2055)
Arctic, March	1993 (1986–N/A)	2004 (N/A–2035)	2034 (2025–2043)
Antarctic, October	1975 (1974–1977)	2085 (2068–2095)	2060 (2055–2066)
Northern midlatitudes	1990 (1986–N/A)	2005 (N/A–2028)	2032 (2020–2044)
Tropics	N/A (1988–N/A)	N/A (N/A–2028)	2058 (2038—N/A)
Southern midlatitudes	1981 (1978–1986)	2039 (2028–2048)	2045 (2039–2050)

Note. N/A indicates that the threshold was not crossed by that percentile.
[a]1980-return dates are the MMM1S for refC2 TCO data reported by Dhomse et al. (2018); their Table 3.

chlorine (EESC) mixing ratios had increased significantly by 1980, TCO trends in the Northern Hemisphere and tropics were initially partially masked by increases in tropospheric column ozone (Shepherd et al., 2014).

To show how simulated S/N ratios in the refC2 simulations compare with observations, we compute S/N ratios for the long-running TCO observational records at Oxford and Arosa (51°N and 46°N, respectively). Note that in calculating S/N for model data, it is unnecessary to baseline-correct data to fit observations as is done when assessing return dates (Dhomse et al., 2018) as change is inherently expressed relative to each model's baseline.

Figure 2 shows that the observed TCO depletion emerges in 1984 at both northern midlatitude stations. This is approximately 5 years before the refC2 multi-model median emerges at Oxford and 8 years earlier at Arosa, but within the 16th and 84th percentiles (which represent approximately one standard deviation on either side of the mean). The delayed emergence of TCO depletion in the CCMI models is at least partially related to tropospheric ozone, which is high-biased at northern midlatitudes in the models (Archibald et al., 2020; Parrish et al., 2014; Revell et al., 2018).

In contrast to the Northern Hemisphere, Antarctic springtime TCO depletion emerges in 1975 (1974–1977; 16th-84th percentiles) in refC2 simulations. Observations show that the depletion of the ozone layer above

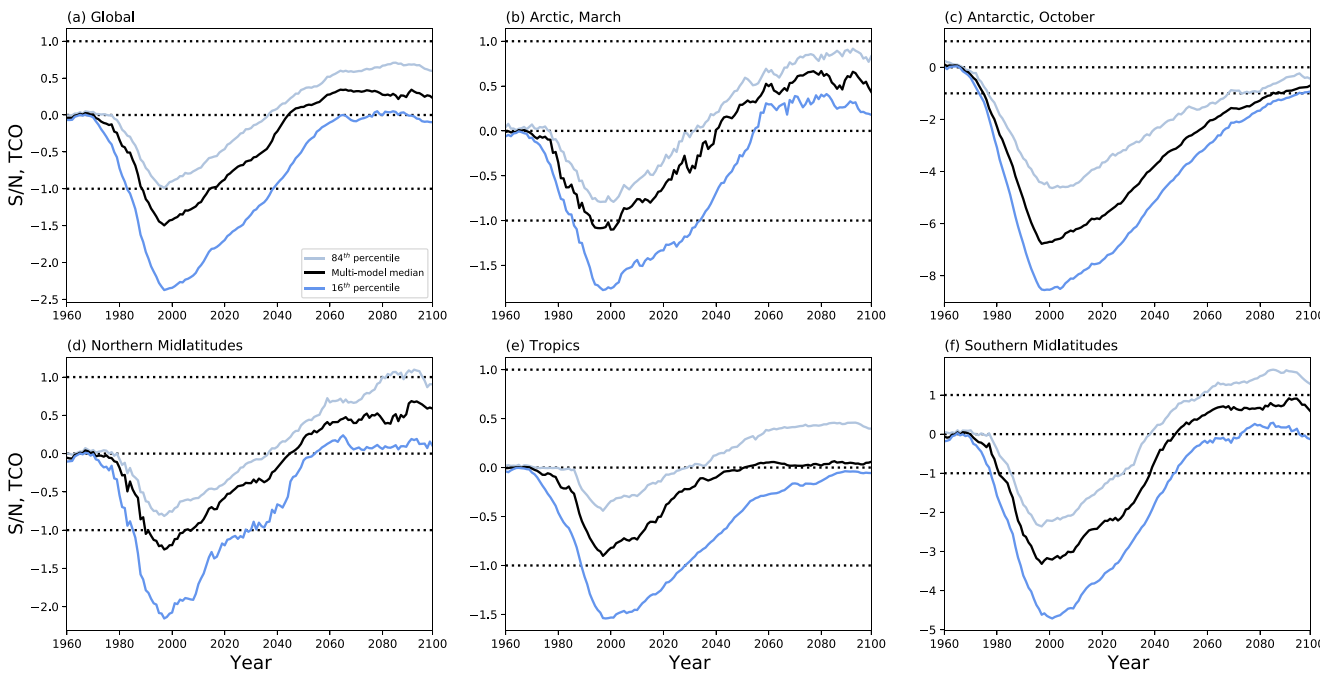

Figure 1. Signal-to-noise ratios in TCO in the refC2 simulations. Black dotted lines show S/N = ±-1 thresholds. S/N ratios are shown for: (a) the global annual mean; (b) the Arctic (60–90°N) in March; (c) the Antarctic (60–90°S) in October; (d) the northern midlatitude (30–60°N) annual mean; (e) the tropical (30°N-30°S) annual mean; (f) the southern midlatitude (30–60°S) annual mean.

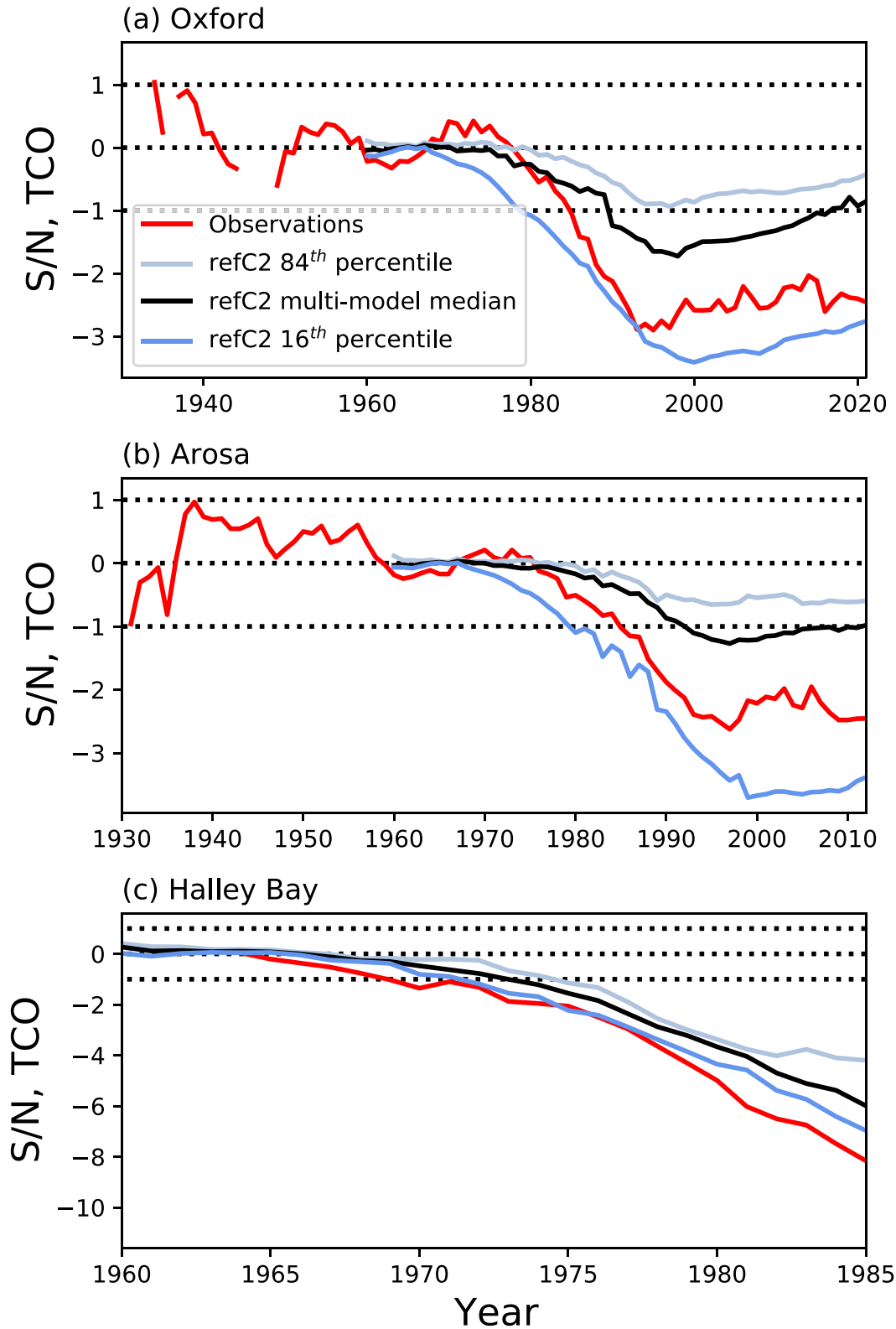

Figure 2. S/N ratios in observed annual-mean TCO in (a) Oxford, United Kingdom (51.75°N, 1.26°W); (b) Arosa, Switzerland (46.78°N, 9.68°E); Halley Bay, Antarctica (75.57°S, 25.52°W). Note that the data span varying date ranges. Corresponding S/N ratios at the 16th, 50th and 84th percentiles from the CCMI refC2 simulations are also shown. Horizontal dotted lines show S/N thresholds of ±-1, which are indicative of a 1σ shift in TCO from the baseline state.

Antarctica was underway between 1960 and 1980 (Farman et al., 1985; Langematz et al., 2016). Indeed, the emergence of TCO depletion in the Halley Bay (Antarctica) observational record is visible in 1968 (Figure 2c). Assessing the effectiveness of the Montreal Protocol by determining whether Antarctic TCO returns to 1980 therefore sets a low threshold for success and, as noted by Langematz et al. (2016), "is not indicative of full recovery of the Antarctic ozone layer from the effects of ODSs."

TCO is projected to increase through the 21st century under the RCP 6.0/WMO (2011) A1 scenario (Figure 1), and indeed, in all moderate-to-high GHG emissions scenarios (Hassler & Young, 2022; Keeble et al., 2021). Some regions show an increase of TCO above 1960–1980 levels (sometimes called a "super-recovery") due to the combined effects of EESC decreasing and GHGs increasing. S/N ratios indicate the de-emergence of TCO depletion ($S/N > -1$) in all regions during the 21st century. This finding is broadly consistent with Dhomse et al. (2018), who reported 1980-return dates for the CCMI refC2 simulations in the 2030s–2060s (Table 1). However, some significant differences exist between the de-emergence years reported here and the 1980-return years by Dhomse et al. (2018). Most notably, Antarctic springtime TCO de-emerges 25 years after its 1980-return date reported by Dhomse et al. (2018); Table 1 and Figure 3. This is because the S/N metric as applied here takes into account the significant Antarctic TCO losses that occurred prior to 1980.

3.2. Using S/N to Assess the Effectiveness of the Montreal Protocol

Interpreting changes in stratospheric ozone by examining TCO is confounded by changes in tropospheric ozone that have occurred in the recent past (Gaudel et al., 2018; Tarasick et al., 2019). To eliminate the tropospheric ozone signal, S/N ratios in SCO are shown in Figure S3 in Supporting Information S1 and emergence and de-emergence dates are given in Table 2. Emergence of SCO depletion is largely consistent with TCO, with the exception of the tropics. Here, SCO depletion emerges between 1977 and 1983 (16th and 84th percentiles). Tropical SCO depletion never de-emerges in the 21st century due to GHG-induced acceleration of the Brewer-Dobson circulation (Butchart & Scaife, 2001).

Because the refC2 simulation includes transient GHG concentrations following the RCP6.0 simulation, analysis of SCO alone does not allow quantification as to when stratospheric ozone will recover from the effects of halogen-containing source gases controlled by the Montreal Protocol. GHGs influence stratospheric ozone via chemical and dynamical processes and/or radiative feedbacks, for example, by producing reactive species in the stratosphere that destroy ozone; accelerating the rate of the Brewer-Dobson circulation, or cooling the stratosphere, which influences temperature-dependent ozone production and destruction reactions (Butchart, 2014; Fleming et al., 2011; Hassler & Young, 2022; Ravishankara et al., 2009; Revell et al., 2012; Rosenfield et al., 2002). Keeble et al. (2021) show that ozone recovery is delayed in low GHG emissions scenarios and note that because GHGs influence stratospheric ozone, the relevance of 1980-return dates to assess the effectiveness of the Montreal Protocol is questionable.

To identify when stratospheric ozone recovers from depletion by halogen-containing source gases controlled by the Montreal Protocol, we calculate S/N ratios for SCO in senC2fGHG simulations. These simulations feature GHGs held at constant 1960 concentrations for the entire length of the simulation. However, tropospheric ozone precursors are identical to the refC2 simulation therefore we analyze SCO to remove the contribution from tropospheric ozone. In most regions, de-emergence of halocarbon-induced stratospheric ozone depletion occurs later in senC2fGHG simulations than in refC2 simulations (Table 2, Figure S4 in Supporting Information S1), and doesn't always occur during the 21st century. In contrast, S/N ratios in tropical SCO show de-emergence occurring between 2046 and 2086 (16th and 84th percentiles) in senC2fGHG simulations: that is, tropical SCO would recover from the effects of halocarbons during the 21st century in the absence of GHG emissions.

It has long been known that 1980-return dates are an oversimplified and arbitrary approach to assessing the effectiveness of the Montreal Protocol. The de-emergence dates calculated here are in some regions statistically significantly different from 1980-return dates (Figure 3), because 1980 does not accurately reflect the onset of significant stratospheric ozone depletion, especially over Antarctica (Farman et al., 1985; Langematz et al., 2016; Shepherd t al., 2014). Because S/N provides an indication of when TCO is no longer statistically significantly different from local (and global, perhaps) unperturbed values, we argue that approaches like the one sketched here are perhaps more suitable metrics for assessing the impact and effectiveness of the Montreal Protocol.

The main advantage of the S/N metric is that it identifies when the variable of interest shifts to a statistically significantly different state from its baseline or "natural" state. A further advantage is that because it is a ratio between signal and noise, baseline correction to observations is unnecessary, making it easy to apply. Unlike new

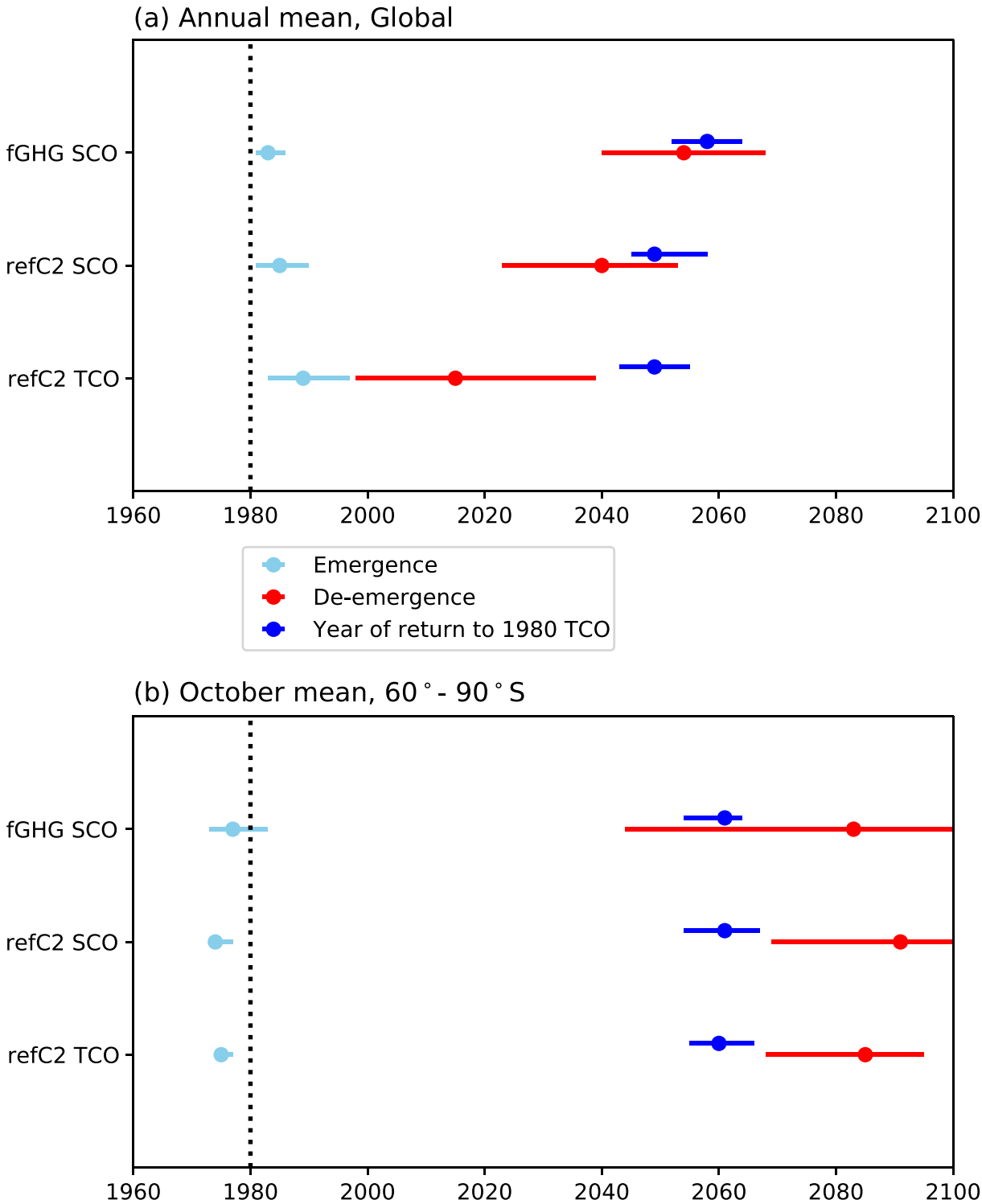

Figure 3. Emergence and de-emergence of TCO and SCO, compared with 1980-return dates reported by Dhomse et al. (2018); their Tables 3 and 4. The 1980-return dates reported are the multi-model mean $\pm 1\sigma$, while the emergence and de-emergence dates are the multi-model median $\pm$ the 16th and 84th percentiles.

metrics such as the Integrated Ozone Depletion (Pyle et al., 2022), it doesn't quantify the total amount of ozone loss but more importantly when statistically significant ozone decreases or increases have occurred.

Many factors could, and are, delaying ozone recovery. These include large wildfires, which will become more frequent and intense in a changing climate (Solomon et al., 2022, 2023; Strahan et al., 2022), major volcanic

Table 2
Emergence and De-Emergence of MMM1S SCO in refC2 Simulations, Represented by the Median Year and the 16th and 84th Percentiles in Brackets

Region	refC2 emergence	senC2fGHG emergence	refC2 de-emergence	senC2fGHG de-emergence
Global-mean	1985 (1980–1990)	1983 (1981–1986)	2040 (2023–2053)	2054 (2040–2068)
Arctic, March	1993 (1983–N/A)	1987 (1981–1995)	2004 (N/A—2039)	2030 (2001–2042)
Antarctic, October	1974 (1973–1978)	1977 (1973–1983)	2091 (2069—N/A)	2083 (2044–N/A)
Northern midlatitudes	1988 (1983–1992)	1981 (1979–1986)	2022 (2005–2047)	2064 (2049–N/A)
Tropics	1980 (1977–1983)	1980 (1978–1985)	N/A (N/A—N/A)	2061 (2046–2086)
Southern midlatitudes	1980 (1976–1982)	1978 (1975–1980)	2047 (2039–2058)	2076 (2060–2097)

eruptions (Lu et al., 2023; Tie & Brasseur, 1995), emissions of currently unregulated ozone-depleting substances (Fang et al., 2019; Ravishankara et al., 2009), and illegal emissions of controlled ozone-depleting substances (Dameris et al., 2019; Montzka et al., 2018). While the Montreal Protocol has been enormously successful in phasing out halogen-containing source gases, the ozone layer is far from a solved problem. It is perhaps concerning that only small ensembles of models with interactive stratospheric chemistry are available from the most up-to-date chemistry-climate models, as the large spread given by these models makes constraining projections for a range of potential future scenarios difficult. While interactive chemistry is computationally expensive, we recommend prioritizing such simulations in future model intercomparison projects.

4. Conclusions

Atmospheric composition and climate are evolving rapidly in the 21st century and numerous processes are affecting stratospheric ozone and how it is affected by stratospheric chlorine. Increasingly used in the climate change literature, we show that S/N is a useful and appropriate metric by which to assess the return of stratospheric ozone abundances to its baseline state.

S/N ratios computed for TCO in CCMI-1 refC2 simulations using 1960–1970 as a baseline noise period show that TCO depletion "emerges" (i.e., S/N < -1, an approximately 1σ shift from the mean) prior to 1980 over Antarctica, and after 1980 almost everywhere else which is partly due to increases in tropospheric ozone partially masking stratospheric ozone losses. As a consequence, global-mean TCO "de-emerges" (S/N > -1) before it would otherwise return to 1980 levels. However, the presence of other drivers of TCO changes, such as GHGs and tropospheric ozone precursors, does not imply that ODSs no longer affect TCO even once a return of TCO to 1980s levels is reached. Large ensembles of models including interactive stratospheric chemistry, should they become available in future model intercomparison efforts, will enable further analysis of S/N ratios in stratospheric ozone and the effectiveness of the Montreal Protocol.

Data Availability Statement

Chemistry-Climate Model Initiative Phase 1 model data used in this study are available from the Centre for Environmental Data Analysis (CEDA; http://data.ceda.ac.uk/badc/wcrp-ccmi/data/CCMI-1/). Ozone data for Arosa are available from the World Ozone and Ultraviolet Radiation Data Centre (WOUDC, https://woudc.org/archive/Archive-NewFormat/TotalOzone_1.0_1/stn035/dobson/). Ozone data for Oxford were taken from the Supporting Data of Brönnimann (2022) and are available from WOUDC (https://woudc.org/archive/Archive-NewFormat/TotalOzone_1.0_1/stn048/dobson/). Ozone data for Halley Bay are provided by the British Antarctic Survey (BAS, https://legacy.bas.ac.uk/met/jds/ozone/index.html#data).

Acknowledgments
This research was supported by the Ministry of Business, Innovation & Employment Endeavor Fund (Contract RTVU1906). The authors acknowledge the modeling groups for making their simulations available for this analysis, the joint WCRP SPARC/IGAC Chemistry-Climate Model Initiative (CCMI) for organizing and coordinating the model data analysis activity, and the Centre for Environmental Data Analysis (CEDA) for collecting and archiving the CCMI model output. Open access publishing facilitated by University of Canterbury, as part of the Wiley - University of Canterbury agreement via the Council of Australian University Librarians.

References

Archibald, A. T., Neu, J. L., Elshorbany, Y. F., Cooper, O. R., Young, P. J., Akiyoshi, H., et al. (2020). Tropospheric ozone assessment report: A critical review of changes in the tropospheric ozone burden and budget from 1850 to 2100. *Elementa: Science of the Anthropocene*, *8*(1). https://doi.org/10.1525/elementa.2020.034

Braesicke, P., Neu, J., & Fioletov, V. (2018). Update on global ozone: Past, present, and future. In *Scientific assessment of ozone depletion: 2018. WMO global ozone Res. Monit. Proj. – Rep.* (Vol. 58(3)), World Meteorol. Organization.

Brönnimann, S. (2022). Century-long column ozone records show that chemical and dynamical influences counteract each other. *Communications Earth & Environment*, *3*(1), 143. https://doi.org/10.1038/s43247-022-00472-z

Brönnimann, S., Staehelin, J., Farmer, S. F. G., Cain, J. C., Svendby, T., & Svenøe, T. (2003). Total ozone observations prior to the IGY. i: A history. *Quarterly Journal of the Royal Meteorological Society*, *129*(593), 2797–2817. https://doi.org/10.1256/qj.02.118

Butchart, N. (2014). The Brewer-Dobson circulation. *Reviews of Geophysics*, *52*(2), 157–184. https://doi.org/10.1002/2013RG000448

Butchart, N., & Scaife, A. A. (2001). Removal of chlorofluorocarbons by increased mass exchange between the stratosphere and troposphere in a changing climate. *Nature*, *410*(6830), 799–802. https://doi.org/10.1038/35071047

Checa-Garcia, R. (2018). *CMIP6 ozone forcing dataset: Supporting information*. Zenodo. https://doi.org/10.5281/zenodo.1135127

Checa-Garcia, R., Hegglin, M. I., Kinnison, D., Plummer, D. A., & Shine, K. P. (2018). Historical tropospheric and stratospheric ozone radiative forcing using the CMIP6 database. *Geophysical Research Letters*, *45*(7), 3264–3273. https://doi.org/10.1002/2017gl076770

Chipperfield, M. P., Bekki, S., Dhomse, S., Harris, N. R. P., Hassler, B., Hossaini, R., et al. (2017). Detecting recovery of the stratospheric ozone layer. *Nature*, *549*(7671), 211–218. https://doi.org/10.1038/nature23681

Coldewey-Egbers, M., Loyola, D. G., Lerot, C., & Van Roozendael, M. (2022). Global, regional and seasonal analysis of total ozone trends derived from the 1995–2020 GTO-ECV climate data record. *Atmospheric Chemistry and Physics*, *22*(10), 6861–6878. https://doi.org/10.5194/acp-22-6861-2022

Dameris, M., Jöckel, P., & Nützel, M. (2019). Possible implications of enhanced chlorofluorocarbon-11 concentrations on ozone. *Atmospheric Chemistry and Physics*, *19*(22), 13759–13771. https://doi.org/10.5194/acp-19-13759-2019

Dhomse, S. S., Kinnison, D., Chipperfield, M. P., Salawitch, R. J., Cionni, I., Hegglin, M. I., et al. (2018). Estimates of ozone return dates from Chemistry-Climate Model Initiative simulations. *Atmospheric Chemistry and Physics*, *18*(11), 8409–8438. https://doi.org/10.5194/acp-18-8409-2018

Douglas, H. C., Harrington, L. J., Joshi, M., Hawkins, E., Revell, L. E., & Frame, D. J. (2023). Changes to population-based emergence of climate change from CMIP5 to CMIP6. *Environmental Research Letters*, *18*(1), 014013. https://doi.org/10.1088/1748-9326/aca91e

Eyring, V., Arblaster, J. M., Cionni, I., Sedláček, J., Perlwitz, J., Young, P. J., et al. (2013). Long-term ozone changes and associated climate impacts in CMIP5 simulations. *Journal of Geophysical Research: Atmospheres*, *118*(10), 5029–5060. https://doi.org/10.1002/jgrd.50316

Eyring, V., Bony, S., Meehl, G. A., Senior, C. A., Stevens, B., Stouffer, R. J., & Taylor, K. E. (2016). Overview of the coupled model intercomparison project phase 6 (CMIP6) experimental design and organization. *Geoscientific Model Development*, *9*(5), 1937–1958. https://doi.org/10.5194/gmd-9-1937-2016

Eyring, V., Cionni, I., Bodeker, G. E., Charlton-Perez, A. J., Kinnison, D. E., Scinocca, J. F., et al. (2010). Multi-model assessment of stratospheric ozone return dates and ozone recovery in CCMVal-2 models. *Atmospheric Chemistry and Physics*, *10*(19), 9451–9472. https://doi.org/10.5194/acp-10-9451-2010

Eyring, V., Lamarque, J.-F., Hess, P., Arfeuille, F., Bowman, K., Chipperfield, M. P., et al. (2013). Overview of IGAC/SPARC Chemistry-Climate Model Initiative (CCMI) community simulations in support of upcoming ozone and climate assessments (Tech. Rep. No. ISSN 1245-4680). *SPARC Newsletter no*, *40*, 48–66.

Fang, X., Pyle, J. A., Chipperfield, M. P., Daniel, J. S., Park, S., & Prinn, R. G. (2019). Challenges for the recovery of the ozone layer. *Nature Geoscience*, *12*(8), 592–596. https://doi.org/10.1038/s41561-019-0422-7

Farman, J. C., Gardiner, B. G., & Shanklin, J. D. (1985). Large losses of total ozone in Antarctica reveal seasonal ClO_x/NO_x interaction. *Nature*, *315*(6016), 207–210. https://doi.org/10.1038/315207a0

Fleming, E. L., Jackman, C. H., Stolarski, R. S., & Douglass, A. R. (2011). A model study of the impact of source gas changes on the stratosphere for 1850–2100. *Atmospheric Chemistry and Physics*, *11*(16), 8515–8541. https://doi.org/10.5194/acp-11-8515-2011

Frame, D., Joshi, M., Hawkins, E., Harrington, L. J., & de Roiste, M. (2017). Population-based emergence of unfamiliar climates. *Nature Climate Change*, *7*(6), 407–411. https://doi.org/10.1038/nclimate3297

Gaudel, A., Cooper, O. R., Ancellet, G., Barret, B., Boynard, A., Burrows, J. P., et al. (2018). Tropospheric ozone assessment report: Present-day distribution and trends of tropospheric ozone relevant to climate and global atmospheric chemistry model evaluation. *Elementa: Science of the Anthropocene*, *6*. https://doi.org/10.1525/elementa.291

Harrington, L. J., Frame, D., King, A. D., & Otto, F. E. L. (2018). How uneven are changes to impact-relevant climate hazards in a 1.5°C world and beyond? *Geophysical Research Letters*, *45*(13), 6672–6680. https://doi.org/10.1029/2018GL078888

Hassler, B., & Young, P. J. (2022). Update on global ozone: Past, present, and future. In *Scientific assessment of ozone depletion: 2022. GAW report No. 278*. In *WMO scientific assessment of ozone depletion: 2022, Chap. 3* (p. 509).

Hawkins, E., Frame, D., Harrington, L., Joshi, M., King, A., Rojas, M., & Sutton, R. (2020). Observed emergence of the climate change signal: From the familiar to the unknown. *Geophysical Research Letters*, *47*(6), e2019GL086259. https://doi.org/10.1029/2019gl086259

Keeble, J., Hassler, B., Banerjee, A., Checa-Garcia, R., Chiodo, G., Davis, S., et al. (2021). Evaluating stratospheric ozone and water vapour changes in CMIP6 models from 1850 to 2100. *Atmospheric Chemistry and Physics*, *21*(6), 5015–5061. https://doi.org/10.5194/acp-21-5015-2021

Langematz, U., Schmidt, F., Kunze, M., Bodeker, G. E., & Braesicke, P. (2016). Antarctic ozone depletion between 1960 and 1980 in observations and chemistry–climate model simulations. *Atmospheric Chemistry and Physics*, *16*(24), 15619–15627. https://doi.org/10.5194/acp-16-15619-2016

Lu, J., Lou, S., Huang, X., Xue, L., Ding, K., Liu, T., et al. (2023). Stratospheric aerosol and ozone responses to the Hunga Tonga-Hunga Ha'apai volcanic eruption. *Geophysical Research Letters*, *50*(4), e2022GL102315. https://doi.org/10.1029/2022GL102315

Masui, T., Matsumoto, K., Hijioka, Y., Kinoshita, T., Nozawa, T., Ishiwatari, S., et al. (2011). An emission pathway for stabilization at 6 Wm^{-2} radiative forcing. *Climatic Change*, *109*(1), 59–76. https://doi.org/10.1007/s10584-011-0150-5

Montzka, S. A., Dutton, G. S., Yu, P., Ray, E., Portmann, R. W., Daniel, J. S., et al. (2018). An unexpected and persistent increase in global emissions of ozone-depleting CFC-11. *Nature*, *557*(7705), 413–417. https://doi.org/10.1038/s41586-018-0106-2

Morgenstern, O., Hegglin, M. I., Rozanov, E., O'Connor, F. M., Abraham, N. L., Akiyoshi, H., et al. (2017). Review of the global models used within phase 1 of the chemistry–climate model initiative (CCMI). *Geoscientific Model Development*, *10*(2), 639–671. https://doi.org/10.5194/gmd-10-639-2017

Morgenstern, O., Stone, K. A., Schofield, R., Akiyoshi, H., Yamashita, Y., Kinnison, D. E., et al. (2018). Ozone sensitivity to varying greenhouse gases and ozone-depleting substances in CCMI-1 simulations [Journal Article]. *Atmospheric Chemistry and Physics*, *18*(2), 1091–1114. https://doi.org/10.5194/acp-18-1091-2018

Parrish, D. D., Lamarque, J. F., Naik, V., Horowitz, L., Shindell, D. T., Staehelin, J., et al. (2014). Long-term changes in lower tropospheric baseline ozone concentrations: Comparing chemistry-climate models and observations at northern midlatitudes. *Journal of Geophysical Research: Atmospheres*, *119*(9), 5719–5736. https://doi.org/10.1002/2013JD021435

Plummer, D., Nagashima, T., Tilmes, S., Archibald, A., Chiodo, G., Fadnavis, S., et al. (2021). CCMI-2022: A new set of chemistry-climate model initiative (CCMI-2) community simulations to update the assessment of models and support upcoming ozone assessment activities (Tech. Rep. No. ISSN 1245-4680). *SPARC Newsletter no*, *57*, 22–30.

Pyle, J. A., Keeble, J., Abraham, N. L., Chipperfield, M. P., & Griffiths, P. T. (2022). Integrated ozone depletion as a metric for ozone recovery. *Nature*, *608*(7924), 719–723. https://doi.org/10.1038/s41586-022-04968-8

Ravishankara, A. R., Daniel, J. S., & Portmann, R. W. (2009). Nitrous oxide (N_2O): The dominant ozone-depleting substance emitted in the 21st century. *Science*, *326*(5949), 123–125. https://doi.org/10.1126/science.1176985

Revell, L. E., Bodeker, G. E., Huck, P. E., Williamson, B. E., & Rozanov, E. (2012). The sensitivity of stratospheric ozone changes through the 21st century to N_2O and CH_4. *Atmospheric Chemistry and Physics*, *12*(23), 11309–11317. https://doi.org/10.5194/acp-12-11309-2012

Revell, L. E., Robertson, F., Douglas, H., Morgenstern, O., & Frame, D. (2022). Influence of ozone forcing on 21st century Southern Hemisphere surface westerlies in CMIP6 models. *Geophysical Research Letters*, *49*(6), e2022GL098252. https://doi.org/10.1029/2022GL098252

Revell, L. E., Stenke, A., Tummon, F., Feinberg, A., Rozanov, E., Peter, T., et al. (2018). Tropospheric ozone in CCMI models and Gaussian process emulation to understand biases in the SOCOLv3 chemistry–climate model. *Atmospheric Chemistry and Physics*, *18*(21), 16155–16172. https://doi.org/10.5194/acp-18-16155-2018

Rosenfield, J. E., Douglass, A. R., & Considine, D. B. (2002). The impact of increasing carbon dioxide on ozone recovery. *Journal of Geophysical Research*, *107*(D6), ACH7-1–ACH7-9. https://doi.org/10.1029/2001JD000824

Shepherd, T. G., Plummer, D. A., Scinocca, J. F., Hegglin, M. I., Fioletov, V. E., Reader, M. C., et al. (2014). Reconciliation of halogen-induced ozone loss with the total-column ozone record. *Nature Geoscience*, *7*(6), 443–449. https://doi.org/10.1038/ngeo2155

Solomon, S., Dube, K., Stone, K., Yu, P., Kinnison, D., Toon, O. B., et al. (2022). On the stratospheric chemistry of midlatitude wildfire smoke. *Proceedings of the National Academy of Sciences*, *119*(10), e2117325119. https://doi.org/10.1073/pnas.2117325119

Solomon, S., Ivy, D. J., Kinnison, D., Mills, M. J., Neely, R. R., & Schmidt, A. (2016). Emergence of healing in the Antarctic ozone layer. *Science*, *353*(6296), 269–274. https://doi.org/10.1126/science.aae0061

Solomon, S., Stone, K., Yu, P., Murphy, D. M., Kinnison, D., Ravishankara, A. R., & Wang, P. (2023). Chlorine activation and enhanced ozone depletion induced by wildfire aerosol. *Nature*, *615*(7951), 259–264. https://doi.org/10.1038/s41586-022-05683-0

Son, S.-W., Han, B.-R., Garfinkel, C. I., Kim, S.-Y., Park, R., Abraham, N. L., et al. (2018). Tropospheric jet response to Antarctic ozone depletion: An update with Chemistry-Climate Model Initiative (CCMI) models. *Environmental Research Letters*, *13*(5), 054024. https://doi.org/10.1088/1748-9326/aabf21

Strahan, S. E., Smale, D., Solomon, S., Taha, G., Damon, M. R., Steenrod, S. D., et al. (2022). Unexpected repartitioning of stratospheric inorganic chlorine after the 2020 Australian wildfires. *Geophysical Research Letters*, *49*(14), e2022GL098290. https://doi.org/10.1029/2022GL098290

Tarasick, D., Galbally, I. E., Cooper, O. R., Schultz, M. G., Ancellet, G., Leblanc, T., et al. (2019). Tropospheric ozone assessment report: Tropospheric ozone from 1877 to 2016, observed levels, trends and uncertainties. *Elementa: Science of the Anthropocene*, *7*. https://doi.org/10.1525/elementa.376

Tie, X., & Brasseur, G. (1995). The response of stratospheric ozone to volcanic eruptions: Sensitivity to atmospheric chlorine loading. *Geophysical Research Letters*, *22*(22), 3035–3038. https://doi.org/10.1029/95GL03057

Weber, M., Arosio, C., Coldewey-Egbers, M., Fioletov, V. E., Frith, S. M., Wild, J. D., et al. (2022). Global total ozone recovery trends attributed to ozone-depleting substance (ODS) changes derived from five merged ozone datasets. *Atmospheric Chemistry and Physics*, *22*(10), 6843–6859. https://doi.org/10.5194/acp-22-6843-2022

World Meteorological Organization. (1957). Definition of the tropopause (Vol. *6*, pp. 136–137).

World Meteorological Organization. (2011). Scientific assessment of ozone depletion: 2010. In *WMO global ozone research and monitoring project – Report No. 52*.

References From the Supporting Information

Akiyoshi, H., Nakamura, T., Miyasaka, T., Shiotani, M., & Suzuki, M. (2016). A nudged chemistry-climate model simulation of chemical constituent distribution at northern high-latitude stratosphere observed by SMILES and MLS during the 2009/2010 stratospheric sudden warming. *Journal of Geophysical Research: Atmospheres*, *121*(3), 1361–1380. https://doi.org/10.1002/2015JD023334

Bednarz, E. M., Maycock, A. C., Abraham, N. L., Braesicke, P., Dessens, O., & Pyle, J. A. (2016). Future Arctic ozone recovery: The importance of chemistry and dynamics. *Atmospheric Chemistry and Physics*, *16*(18), 12159–12176. https://doi.org/10.5194/acp-16-12159-2016

Deushi, M., & Shibata, K. (2011). Development of a Meteorological Research Institute chemistry-climate model version 2 for the study of tropospheric and stratospheric chemistry. *Papers in Meteorology and Geophysics*, *62*, 1–46. https://doi.org/10.2467/mripapers.62.1

Guth, J., Josse, B., Marécal, V., Joly, M., & Hamer, P. (2016). First implementation of secondary inorganic aerosols in the MOCAGE version 2.15.0 chemistry transport model. *Geoscientific Model Development*, *9*(1), 137–160. https://doi.org/10.5194/gmd-9-137-2016

Hardiman, S. C., Butchart, N., O'Connor, F. M., & Rumbold, S. T. (2017). The Met Office HadGEM3-ES chemistry–climate model: Evaluation of stratospheric dynamics and its impact on ozone. *Geoscientific Model Development*, *10*(3), 1209–1232. https://doi.org/10.5194/gmd-10-1209-2017

Imai, K., Manago, N., Mitsuda, C., Naito, Y., Nishimoto, E., Sakazaki, T., et al. (2013). Validation of ozone data from the superconducting submillimeter-wave limb-emission sounder (SMILES). *Journal of Geophysical Research: Atmospheres*, *118*(11), 5750–5769. https://doi.org/10.1002/jgrd.50434

Jonsson, A. I., de Grandpré, J., Fomichev, V. I., McConnell, J. C., & Beagley, S. R. (2004). Doubled CO_2-induced cooling in the middle atmosphere: Photochemical analysis of the ozone radiative feedback. *Journal of Geophysical Research*, *109*(D24), D24103. https://doi.org/10.1029/2004JD005093

Josse, B., Simon, P., & Peuch, V. H. (2004). Radon global simulations with the multiscale chemistry and transport model MOCAGE. *Tellus B: Chemical and Physical Meteorology*, *56*(4), 339–356. https://doi.org/10.3402/tellusb.v56i4.16448

Jöckel, P., Kerkweg, A., Pozzer, A., Sander, R., Tost, H., Riede, H., et al. (2010). Development cycle 2 of the modular Earth submodel system (MESSy2). *Geoscientific Model Development*, *3*(2), 717–752. https://doi.org/10.5194/gmd-3-717-2010

Jöckel, P., Tost, H., Pozzer, A., Kunze, M., Kirner, O., Brenninkmeijer, C. A. M., et al. (2016). Earth system chemistry integrated modelling (ESCiMo) with the modular Earth submodel system (MESSy) version 2.51. *Geoscientific Model Development*, *9*(3), 1153–1200. https://doi.org/10.5194/gmd-9-1153-2016

Michou, M., Saint-Martin, D., Teyssèdre, H., Alias, A., Karcher, F., Oliviè, D., et al. (2011). A new version of the CNRM chemistry-climate model, CNRM-CCM: Description and improvements from the CCMVal-2 simulations. *Geoscientific Model Development*, *4*(4), 873–900. https://doi.org/10.5194/gmd-4-873-2011

Molod, A., Takacs, L., Suarez, M., & Bacmeister, J. (2015). Development of the GEOS-5 atmospheric general circulation model: Evolution from MERRA to MERRA2. *Geoscientific Model Development*, *8*(5), 1339–1356. https://doi.org/10.5194/gmd-8-1339-2015

Morgenstern, O., Braesicke, P., O'Connor, F. M., Bushell, A. C., Johnson, C. E., Osprey, S. M., & Pyle, J. A. (2009). Evaluation of the new UKCA climate-composition model – Part 1: The stratosphere. *Geoscientific Model Development*, *2*(1), 43–57. https://doi.org/10.5194/gmd-2-43-2009

Morgenstern, O., Zeng, G., Luke Abraham, N., Telford, P. J., Braesicke, P., Pyle, J. A., et al. (2013). Impacts of climate change, ozone recovery, and increasing methane on surface ozone and the tropospheric oxidizing capacity. *Journal of Geophysical Research: Atmospheres*, *118*(2), 1028–1041. https://doi.org/10.1029/2012JD018382

O'Connor, F. M., Johnson, C. E., Morgenstern, O., Abraham, N. L., Braesicke, P., Dalvi, M., et al. (2014). Evaluation of the new UKCA climate-composition model – Part 2: The troposphere. *Geoscientific Model Development*, *7*(1), 41–91. https://doi.org/10.5194/gmd-7-41-2014

Oman, L. D., Douglass, A. R., Ziemke, J. R., Rodriguez, J. M., Waugh, D. W., & Nielsen, J. E. (2013). The ozone response to ENSO in Aura satellite measurements and a chemistry-climate simulation. *Journal of Geophysical Research: Atmospheres*, *118*(2), 965–976. https://doi.org/10.1029/2012JD018546

Pitari, G., Aquila, V., Kravitz, B., Robock, A., Watanabe, S., Cionni, I., et al. (2014). Stratospheric ozone response to sulfate geoengineering: Results from the geoengineering model intercomparison project (GeoMIP). *Journal of Geophysical Research: Atmospheres*, *119*(5), 2629–2653. https://doi.org/10.1002/2013JD020566

Revell, L. E., Tummon, F., Stenke, A., Sukhodolov, T., Coulon, A., Rozanov, E., et al. (2015). Drivers of the tropospheric ozone budget throughout the 21st century under the medium-high climate scenario RCP 6.0. *Atmospheric Chemistry and Physics*, *15*(10), 5887–5902. https://doi.org/10.5194/acp-15-5887-2015

Scinocca, J. F., McFarlane, N. A., Lazare, M., Li, J., & Plummer, D. (2008). Technical note: The CCCma third generation AGCM and its extension into the middle atmosphere. *Atmospheric Chemistry and Physics*, *8*(23), 7055–7074. https://doi.org/10.5194/acp-8-7055-2008

Stenke, A., Schraner, M., Rozanov, E., Egorova, T., Luo, B., & Peter, T. (2013). The SOCOL version 3.0 chemistry–climate model: Description, evaluation, and implications from an advanced transport algorithm. *Geoscientific Model Development*, *6*(5), 1407–1427. https://doi.org/10.5194/gmd-6-1407-2013

Stone, K. A., Morgenstern, O., Karoly, D. J., Klekociuk, A. R., French, W. J., Abraham, N. L., & Schofield, R. (2016). Evaluation of the ACCESS – Chemistry–climate model for the Southern Hemisphere. *Atmospheric Chemistry and Physics*, *16*(4), 2401–2415. https://doi.org/10.5194/acp-16-2401-2016

Sudo, K., Takahashi, M., Kurokawa, J.-i., & Akimoto, H. (2002). CHASER: A global chemical model of the troposphere 1. Model description. *Journal of Geophysical Research*, *107*(D17), ACH7-1–ACH7-20. https://doi.org/10.1029/2001JD001113

Voldoire, A., Sanchez-Gomez, E., Salas y Mélia, D., Decharme, B., Cassou, C., Sénési, S., et al. (2013). The CNRM-CM5.1 global climate model: Description and basic evaluation. *Climate Dynamics*, *40*(9), 2091–2121. https://doi.org/10.1007/s00382-011-1259-y

Watanabe, S., Hajima, T., Sudo, K., Nagashima, T., Takemura, T., Okajima, H., et al. (2011). MIROC-ESM 2010: Model description and basic results of CMIP5-20c3m experiments. *Geoscientific Model Development*, *4*(4), 845–872. https://doi.org/10.5194/gmd-4-845-2011

Yukimoto, S., Adachi, Y., Hosaka, M., Sakami, T., Yoshimura, H., Hirabara, M., et al. (2012). A new global climate model of the meteorological research institute: MRI-CGCM3: Model description and basic performance. *Journal of the Meteorological Society of Japan. Ser. II*, *90A*, 23–64. https://doi.org/10.2151/jmsj.2012-A02